



PII S0735-1933(99)00058-5

## MIXED CONVECTION EFFECTS ON UNSTEADY FLOW AND HEAT TRANSFER OVER A STRETCHED SURFACE

Ali J. Chamkha<sup>1</sup> and Camille Issa<sup>2</sup>

<sup>1</sup>Department of Mechanical and Industrial Engineering  
Kuwait University  
Safat, 13060 KUWAIT

<sup>2</sup>Department of Civil Engineering  
Lebanese American University  
Byblos - LEBANON

(Communicated by J.P. Hartnett and W.J. Minkowycz)

### ABSTRACT

This work focuses on the effects of mixed convection currents on the problem of unsteady, laminar, boundary-layer flow and heat transfer of an electrically-conducting and heat generating or absorbing fluid over a semi-infinite vertical stretched surface in the presence of a uniform magnetic field. The surface is assumed to be permeable so that to account for possible fluid wall suction or injection and that it is maintained at a variable power-law temperature and is being stretched with a linear velocity with the distance along the surface. The governing equations are derived based on the boundary-layer theory and using the Boussinesq approximation. An appropriate transformation is employed and the transformed equations are solved numerically using the finite-difference method. Comparisons with previously published work are performed and the results are found to be in excellent agreement. A comprehensive parametric study is conducted and a representative set of graphical results for the velocity and temperature profiles as well as the time development of the skin-friction and wall heat transfer coefficients are reported and discussed. © 1999 Elsevier Science Ltd

### Introduction

The boundary-layer flow and heat transfer situation resulting from a continuously stretched vertical surface finds application in a number of manufacturing, technological and engineering processes. For example, materials manufactured by extrusion processes and heat-treated

materials travelling between a feed roll and a wind-up roll or on a conveyor belt possess the characteristics of a continuously moving surface (Vajravelu and Hadjinicolaou [1]). Other examples of these processes include glass blowing, continuous casting, cooling of metallic sheets, cooling of electronic chips, crystal growing, melt spinning and many others.

The classical problem of steady flow on a stretched surface extruded from a slit was first considered by Sakiadis [2,3] who developed a numerical solution using a similarity transformation. Erickson et al. [4] have extended the work of Sakiadis [2] by including fluid suction or injection at the stretched surface and investigating its effects on the heat and mass transfer in the boundary layer. Since then, many other investigators have reported on the steady-state flow from a stretched surface moving with a velocity linearly proportional to the distance along the surface and maintained at various wall thermal conditions (see, for instance, Crane [5], Grubka and Bobba [6]). Vajravelu and Hadjinicolaou [1] have studied convective heat transfer in an electrically-conducting and heat generating fluid from a linearly stretching surface with a uniform free stream. Banks [7] and Ali [8,9] have considered power-law velocity variation of the stretched surface with its tangential distance. Chiam [10] has reported solutions for steady hydromagnetic flow over a surface stretching with a power-law velocity with the distance along the surface.

All of the above investigations have been restricted to steady-state conditions. However, in certain practical problems, the motion of the stretched surface may start impulsively from rest. In these problems the transient or unsteady aspects become of interest. There have been some work done on unsteady flow due to a stretching flat surface (see, for example, Surma Devi et al. [11] and Lakshmish et al. [12], Takhar and Nath [13], Pop and Na [14] and Chamkha [15]). Lately, hydromagnetic flow and heat transfer problems have become more important industrially. For example, and as mentioned by Vajravelu and Hadjinicolaou [1], in many metallurgical processes such as drawing, annealing and tinning of copper wires which involve a cooling stage, the desired characteristics of the final product can be controlled by drawing the material through an electrically-conducting fluid subjected to a magnetic field. In addition, heat generation or absorption effects become significant in some applications such as those dealing with chemical reactions, cooling of electronic equipments, and heat rejection processes. Examples of works on continuously moving surfaces and dealing with either hydromagnetic effects or heat generation or absorption effects or both can be found in the papers by Chakrabarti and Gupta [16], Takhar et al. [17], Kumari et al. [18], Vajravelu and Rollins [19], Vajravelu and Hadjinicolaou [1], and Chamkha [20].

The effects of thermal buoyancy on the unsteady flow and heat transfer characteristics of a stretched permeable surface in the presence of hydromagnetic and heat generation or absorption

effects have not been studied. Therefore, this is the objective of this work. The surface velocity and temperature are assumed to vary linearly with the distance along the surface. In addition, the flow is assumed laminar and the magnetic Reynolds number is assumed to be small so that the induced magnetic field can be neglected.

### Governing Equations

Consider unsteady, incompressible, hydromagnetic, mixed convection, boundary-layer flow of an electrically-conducting and heat-generating or absorbing fluid over a non-isothermal vertical permeable surface stretched with a linear velocity with the distance along the surface. A uniform magnetic field is applied in the direction normal to the surface. The coordinate system is such that  $x$  represents the vertical distance or the distance along the surface and  $y$  represents the horizontal distance or the distance normal to the surface. The governing equations for this problem are based on the balance laws of mass, linear momentum, and energy modified to account for the presence of the magnetic field, thermal buoyancy, wall suction or injection, and the heat generation or absorption effects. These can be written as

$$\frac{\partial u}{\partial x} + \frac{\partial v}{\partial y} = 0 \quad (1)$$

$$\frac{\partial u}{\partial t} + u \frac{\partial u}{\partial x} + v \frac{\partial u}{\partial y} = \nu \frac{\partial^2 u}{\partial y^2} + g\beta(T - T_\infty) - \frac{\sigma}{\rho} B_0^2 u \quad (2)$$

$$\frac{\partial T}{\partial t} + u \frac{\partial T}{\partial x} + v \frac{\partial T}{\partial y} = \alpha \frac{\partial^2 T}{\partial y^2} + \frac{Q_0}{\rho c} (T - T_\infty) \quad (3)$$

where  $t$ ,  $x$  and  $y$  represent time, tangential distance or distance along the surface, and normal distance, respectively.  $u$ ,  $v$ , and  $T$  are the fluid tangential velocity, normal velocity, and temperature, respectively.  $\nu$ ,  $\rho$ ,  $\sigma$ , and  $c$  are the fluid kinematic viscosity, density, electrical conductivity, and specific heat, respectively.  $\beta$  and  $g$  are the thermal expansion coefficient and the acceleration due to gravity, respectively.  $B_0$ ,  $T_\infty$ ,  $\alpha$ , and  $Q_0$  are the magnetic induction, ambient temperature, thermal diffusivity of the fluid, and the dimensional heat generation or absorption coefficient, respectively. It should be mentioned here that positive values of  $Q_0$  indicate heat generation (source) and negative values of  $Q_0$  correspond to heat absorption (sink).

The corresponding initial and boundary conditions for this problem can be written as

$$\begin{aligned}
 u(0, x, y) &= ax, \quad v(0, x, y) = 0, \quad T(0, x, y) = T_\infty + Ax \\
 u(t, x, 0) &= ax, \quad v(t, x, 0) = -v_0, \quad T(t, x, 0) = T_w = T_\infty + Ax \\
 u(t, x, \infty) &= 0, \quad T(t, x, \infty) = T_\infty
 \end{aligned}
 \tag{4}$$

where “a” and A are positive constants and  $v_0 (>0)$  is the suction velocity.

The governing equations are nondimensionalized and transformed by substituting the following dimensionless variables

$$\begin{aligned}
 t &= \frac{\tau}{a}, \quad y = 2\sqrt{\nu t} \eta, \quad u = ax \frac{\partial f}{\partial \eta}(\tau, \eta) \\
 v &= -2a\sqrt{\nu t} f(\tau, \eta), \quad T = T_\infty + (T_w - T_\infty) \theta(\tau, \eta)
 \end{aligned}
 \tag{5}$$

into Equations (1) through (3) to give

$$f''' + 2\eta f'' - 4\tau \frac{\partial f'}{\partial \tau} + 4a\tau(ff'' - (f')^2 - M^2 f' + \frac{Gr}{Re^2} \theta) = 0
 \tag{6}$$

$$\theta'' + Pr(2\eta\theta' - 4\tau \frac{\partial \theta}{\partial \tau} + 4a\tau(f\theta' - f\theta - \phi\theta)) = 0
 \tag{7}$$

with Equation (1) being identically satisfied. In Equations (6) and (7), a prime indicates differentiation with respect to  $\eta$  and  $M = B_0 \sqrt{\sigma / (\rho a)}$ ,  $\phi = Q_0 / (\rho ca)$ ,  $Gr = g\beta(T_w - T_\infty)x^3/\nu^2$ , and  $Re = ax^2/\nu$  are the Hartmann number, the dimensionless heat generation or absorption coefficient, the Grashof number, and the Reynolds number, respectively.

The transformed initial and boundary conditions become

$$\begin{aligned}
 f'(0, \eta) &= 1, \quad f(0, \eta) = 0, \quad \theta(0, \eta) = 1 \\
 f'(\tau, 0) &= 1, \quad f(\tau, 0) = f_0, \quad \theta(\tau, 0) = 1 \\
 f'(\tau, \infty) &= 0, \quad \theta(\tau, \infty) = 0
 \end{aligned}
 \tag{8}$$

where  $f_0 = v_0 / (2a\sqrt{\nu\tau})$  is the dimensionless wall normal velocity such that  $f_0 > 0$  represents suction and  $f_0 < 0$  represents injection at the surface.

Of special significance for this type of flow are the skin-friction coefficient and the wall heat transfer coefficient. These physical parameters can be defined in dimensionless form as

$$C = \frac{-\mu \frac{\partial u}{\partial y} \Big|_{y=0}}{\mu a x} = -f''(\tau, 0) \quad , \quad q = \frac{-k \frac{\partial T}{\partial y} \Big|_{y=0}}{k(T_w - T_\infty)} = -\theta'(\tau, 0) \quad (9a, b)$$

where  $k$  is the thermal conductivity of the fluid.

### Results and Discussion

The initial-value problem represented by Equations (6) through (8) is nonlinear and must be solved numerically. Since the standard, implicit, iterative, finite-difference method discussed by Blottner [21] has proven to be successful at producing accurate results for this type of equations, it is adopted in the present work.

The computational domain is divided into 196 by 196 nodes in the  $\tau$  and  $\eta$  directions, respectively. Since the changes in the dependent variables are expected to be significant in the immediate vicinity of the surface while these changes decrease significantly as the distance far from the wall increases, variable step sizes in the  $\eta$  direction are used. For the same reasons, variable step sizes in the  $\tau$  direction are also employed. The initial step sizes employed were  $\Delta\eta_1 = 0.001$  and  $\Delta\tau_1 = 0.001$  and the growth factors were  $K_\eta = 1.03$  and  $K_\tau = 1.03$  such that  $\Delta\eta_n = K_\eta \Delta\eta_{n-1}$  and  $\Delta\tau_m = K_\tau \Delta\tau_{m-1}$ . The convergence criterion required that the difference between the current and the previous iterations be  $10^{-5}$  in the present work. In this numerical method, the governing equations are linearized by proper evaluation of non-linear terms at the previous iteration. Backward-difference approximations are used for the first derivatives with respect to  $\tau$  while the second-order differential equations are replaced by three-point central-difference quotients. As a result, linear algebraic equations are obtained at each line of constant  $\tau$ . These equations are then solved by the well known Thomas algorithm. For more details on the numerical procedure, the reader is advised to read the paper by Blottner [21].

Figures 1 and 2 present typical steady-state velocity  $f'$  and temperature  $\theta$  profiles for various values of the mixed convection parameter  $Gr/Re^2$ , respectively. For convenience, the value of "a" is set to unity in these and all subsequent figures. The case in which  $Gr/Re^2 = 0$  corresponds to the forced-convection regime while that in which  $Gr/Re^2$  is very large ( $Gr/Re^2 = 100$ ) corresponds to the free-convection regime. The presence of the thermal buoyancy effects represented by finite values of  $Gr/Re^2$  ( $Gr/Re^2 \neq 0$ ) has the tendency to induce more flow along the surface at the expense of small reduction in temperature. This is reflected in the increases in  $f'$  and slight decreases in  $\theta$  as  $Gr/Re^2$  increases shown in Figures 1 and 2, respectively.

Distinctive peaks in the velocity profiles which are characteristics of free-convection flows are also observed for large values of the mixed-convection parameter  $Gr/Re^2$  in Figure 1.

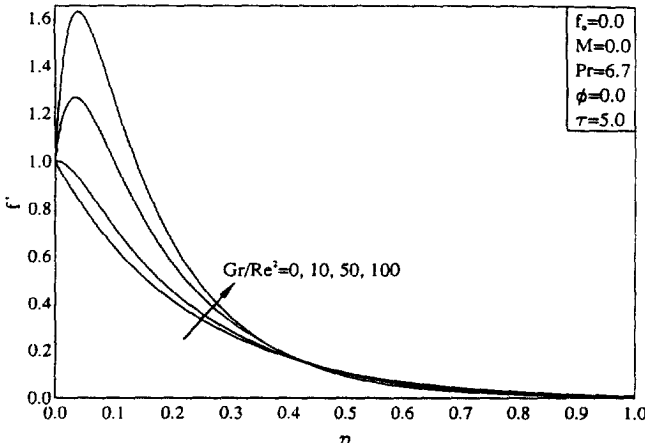


FIG. 1  
Effects of  $Gr/Re^2$  on Velocity Profiles

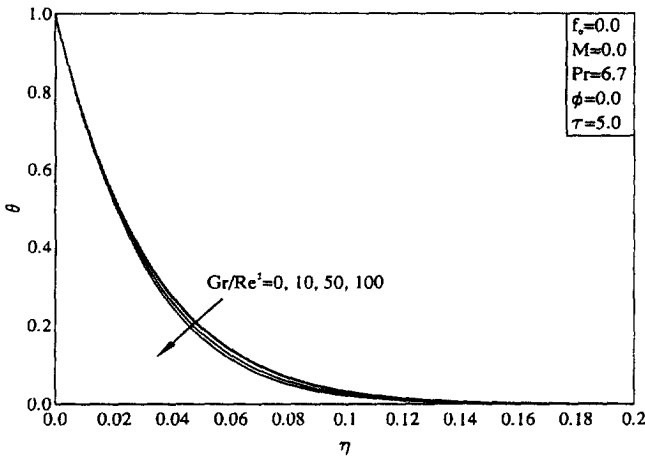


FIG. 2  
Effects of  $Gr/Re^2$  on Temperature Profiles

Figures 3 and 4 depict time histories for the skin-friction coefficient  $C$  and the wall heat transfer  $q$  for various values of the mixed-convection parameter  $Gr/Re^2$ , respectively. For convenience, all the results for  $C$  and  $q$  in these and all subsequent figures are divided by the factor  $2\sqrt{\tau}$ . As observed from Figures 1 and 2, while the slopes of the velocity profiles at the wall increases as  $Gr/Re^2$  increases, the wall slopes of the temperature profiles remain almost constant. This produces reductions in the skin-friction coefficient for all times ( $\tau > 0$ ) as  $Gr/Re^2$  increases while the wall heat transfer remains almost unchanged. Also, and as expected, both the

wall shear stress and heat transfer decrease as  $\tau$  increases. These facts are evident from Figures 3 and 4. It is worth noting that in the absence of the effects of bouyancy ( $Gr/Re^2 = 0$ ), magnetic field ( $M=0$ ), and wall suction or injection ( $f_0 = 0$ ), the steady and unsteady flow solutions were roughly compared with those of Pop and Na [14] and were found to be in excellent agreement.

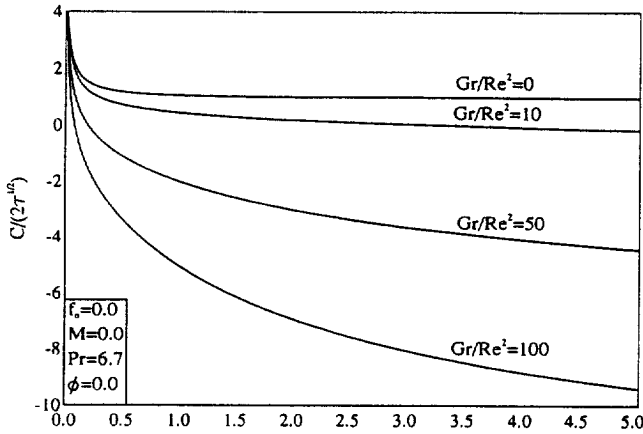


FIG. 3  
Effects of  $Gr/Re^2$  on Skin-Friction Coefficient Time History

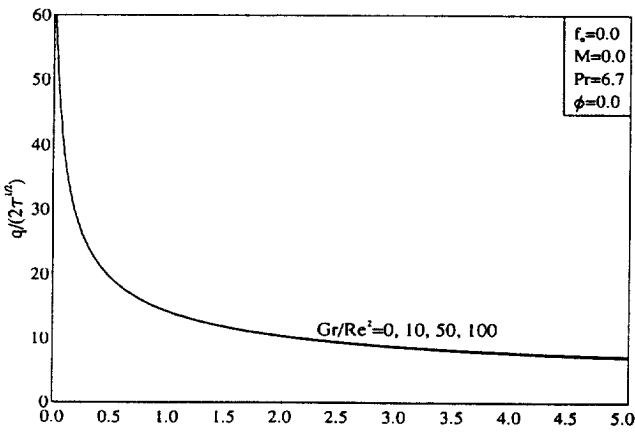


FIG. 4  
Effects of  $Gr/Re^2$  on Wall Heat Transfer Coefficient Time History

Figures 5 and 6 illustrate the effects of the suction or injection parameter  $f_0$ , the Hartmann number  $M$ , the Prandtl number  $Pr$ , and the heat generation or absorption coefficient  $\phi$  on the velocity and temperature profiles, respectively. The parametric conditions for each curve appearing in these and all subsequent figures are given in Table 1. Imposition of fluid suction ( $f_0 > 0$ ) at the wall causes a reduction in the flow velocity along the surface as well as in the flow

temperature. On the other hand injection of fluid at the surface produces the opposite effect , namely increases in both the flow velocity and temperature. These behaviours are reflected by the decreases in  $f'$  and  $\theta$  as  $f_0$  increases shown in Figures 5 and 6. As for the effect of the magnetic field, it is known by now that application of a magnetic field in the direction normal to the flow produces reductions in the flow velocity and increases in its temperature. This is depicted by the decreases in  $f'$  and increases in  $\theta$  as  $M$  increases displayed in Figures 5 and 6. These figures also show that as the heat generation or absorption coefficient  $\phi$  increases, the flow temperature decreases causing a reduction in the flow velocity. However, as the Prandtl number  $Pr$  increases, the flow temperature and, therefore, the flow velocity decreases.

TABLE 1  
Parametric Conditions for Curves in Figures 5 through 8.

Curve	$f_0$	$M$	$Pr$	$\phi$
I	0	0	6.7	0
II	0	3	6.7	0
III	-1	0	6.7	0
IV	1	0	6.7	0
V	0	0	6.7	-1
VI	0	0	6.7	1
VII	0	0	10	0

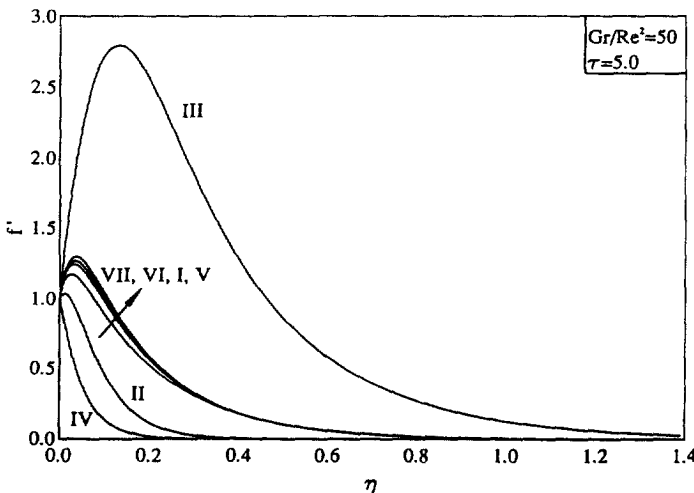


FIG. 5  
Effects of  $f_0$ ,  $M$ ,  $Pr$  and  $\phi$  on Velocity Profiles



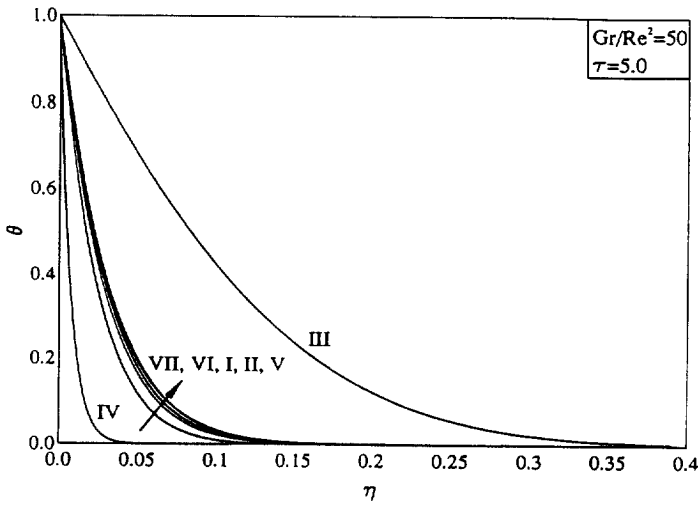


FIG. 6  
Effects of  $f_0$ ,  $M$ ,  $Pr$  and  $\phi$  on Temperature Profiles

The influence of  $f_0$ ,  $M$ ,  $Pr$  and  $\phi$  on the skin-friction and wall heat transfer coefficients are displayed in Figures 7 and 8, respectively. It is seen that both the skin-friction and wall heat transfer coefficients increase as either  $f_0$ ,  $M$ ,  $Pr$  or  $\phi$  increases. It is worth noting that for the case of suction ( $f_0 > 0$ ) both  $C$  and  $q$  initially decrease and later increase as time progresses.

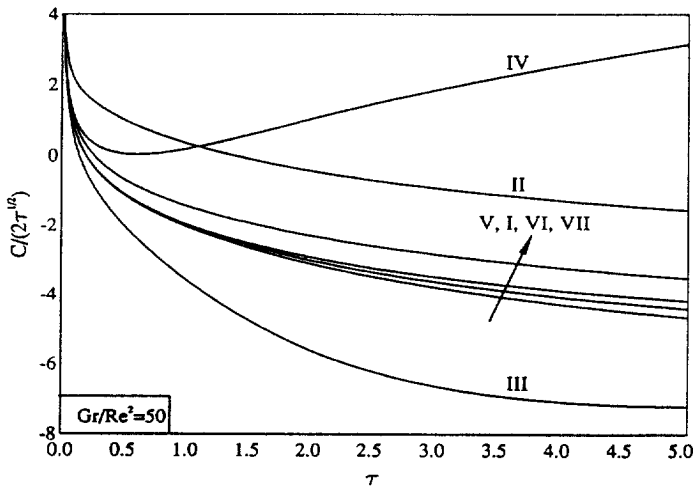


FIG. 7  
Effects of  $f_0$ ,  $M$ ,  $Pr$  and  $\phi$  on Skin-Friction Coefficient Time History

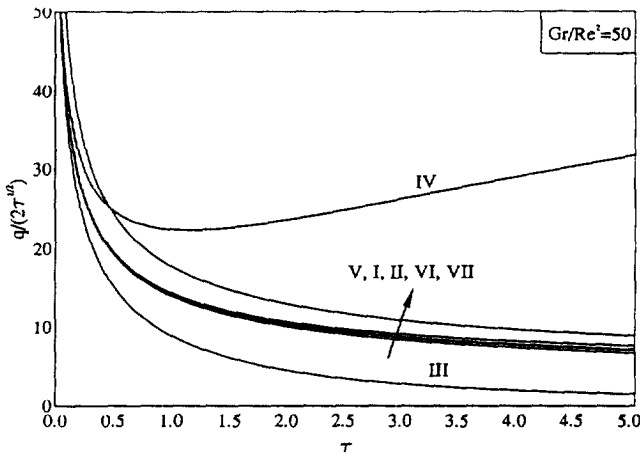


FIG. 8

Effects of  $f_0$ ,  $M$ ,  $Pr$  and  $\phi$  on Wall Heat Transfer Coefficient Time History

### Conclusion

This work focused on the buoyancy and wall suction or injection effects on the problem of unsteady, laminar, hydromagnetic mixed convection boundary-layer flow of an electrically-conducting and heat-generating or absorbing fluid over a non-isothermal vertical stretching permeable surface. The governing equations are transformed and solved numerically by an implicit finite-difference method. Comparisons with previously published work were performed and the results are found to be in excellent agreement. It was found that the wall shear stress increased as either of the Hartmann number, wall suction velocity, or the heat generation coefficient increased while it decreased as the mixed convection parameter increased. In addition, the wall heat transfer was increased as either of the Prandtl number, Hartmann number, surface suction velocity or the heat generation coefficient was increased. However, the surface heat transfer remained almost constant as the mixed convection parameter changed.

### References

1. K. Vajravelu and A. Hadjinicolaou, *Int. J. Engng. Sci.* **35**, 1237 (1977).
2. B.C. Sakiadis, *AIChE J.* **7**, 26 (1961a).
3. B.C. Sakiadis, *AIChE J.* **7**, 221 (1961b).
4. L. E. Erickson, L. T. Fan, and V. G. Fox, *Industrial Engineering and Chemical Fundamentals* **5**, 19 (1966).

5. L.J. Crane, *Z. Angew. Math. Phys.* **21**, 645 (1970).
6. L.G. Grubka and K.M. Bobba, *J. Heat Transfer* **107**, 248 (1985).
7. W.H.H. Banks, *J. Mécanique Théorique et Appliquée* **2**, 375 (1983).
8. M.E. Ali, *J. King Saud Univ.* **8**, Eng. Sci. No. 1, (in press).
9. M.E. Ali, *Int. J. Heat and Fluid Flow* **16**, 280 (1995).
10. T.C. Chiam, *Int. J. Engng. Sci.* **33**, 429 (1995).
11. C.D. Surma Devi, H.S. Takhar and G. Nath, *Int. J. Heat Mass Transfer* **29**, 1996 (1986).
12. K.N. Lakshmisha, S. Venkateswaran and G. Nath, *J. Heat Transfer* **110**, 590 (1988).
13. H.S. Takhar and G. Nath, *Mech. Res. Commun.* **23**, 325 (1996).
14. I. Pop and T.-Y. Na, *Mech. Res. Commun.* **23**, 413 (1996).
15. A. J. Chamkha, *Int. Commun. Heat Mass Transfer*, in press (1998).
16. A. Chakrabarti and A. S. Gupta, *Quart. Appl. Math.* **37**, 73 (1979).
17. H. S. Takhar, A. A. Raptis and A. A. Perdikis, *Acta Mechanica* **65**, 287 (1987).
18. M. Kumari, H. S. Takhar, and G. Nath, *Warme-und Stoffubertr* **25**, 331 (1990).
19. K. Vajravelu and D. Rollins, *Int. J. Non-Linear Mech.* **27**, 265 (1992).
20. A. J. Chamkha, *Int. J. Heat and Fluid Flow*, in press (1998).
21. F. G. Blottner, *AIAA J.* **8**, 193 (1970).

*Received November 12, 1998*